

PHYSICS AND TECHNIQUE OF ACCELERATORS

Research and Design of a New RFQ Injector for Modernization of the LU-20 Drift-Tube Linac

M. A. Gusarova^a, V. S. Dyubkov^a, S. M. Polozov^{a,*}, A. V. Samoshin^a, T. V. Kulevoy^{a,b},
A. A. Martynov^{a,b}, A. S. Plastun^{a,b}, V. A. Andreev^b, S. V. Barabin^b, A. V. Kozlov^b, V. A. Koshelev^b,
G. N. Kropachev^b, R. P. Kuibeda^b, V. G. Kuzmichev^b, D. A. Liakin^b, A. Yu. Orlov^b, D. N. Seleznev^b,
A. L. Sitnikov^b, Yu. B. Stasevich^b, V. S. Aleksandrov^c, A. V. Butenko^c, A. I. Govorov^c, B. V. Golovensky^c,
V. V. Kobets^c, A. D. Kovalenko^c, K. A. Levterov^c, V. A. Monchinsky^c, V. V. Seleznev^c, A. O. Sidorin^c,
G. V. Trubnikov^c, K. A. Klykov^d, I. V. Mamaev^d, M. Yu. Naumenko^d, and G. V. Ostashkov^d

^aNational Research Nuclear University MEPhI, Moscow, Russia

^bInstitute of Theoretical and Experimental Physics, NRC “Kurchatov Institute”, Moscow, Russia

^cJoint Institute for Nuclear Research, Dubna, Russia

^dZababakhin Institute of Technical Physics, Snezhinsk, Russia

*e-mail: smpolozov@mephi.ru

Received February 29, 2016

Abstract—A new NICA heavy-ion collider is now under construction at JINR. At the same time, the Nuclotron facility is being modernized. A joint team from the JINR, MEPhI, and ITEP are now reconstructing a proton and light-ion injection system. New results of the RFQ linac resonator testing and measurements and RF power load are discussed in this article.

DOI: 10.1134/S1547477116070256

INTRODUCTION

The proton and light-ion injection system is now being modernized at JINR as part of a project on constructing a new NICA collider [1]. In particular, the pulsed high-voltage injector of the LU-20 drift-tube linac is going to be replaced with a Radio Frequency Quadrupole (RFQ). The linac equipped with RFQ should ensure the acceleration of ions with the ratio of charge (Z) to mass (A) $0.3 \leq Z/A \leq 0.5$ to the energy 0.156 MeV/n with a current of up to 20 mA and with a current transmission coefficient no worse than 80%. The phase duration of a bunch at the linac output should not exceed 90° and the longitudinal momentum spread should be $\pm 4\%$. The results of modeling beam dynamics and researching and optimizing the electrodynamic properties of the resonator, as well as the resonator design features, are described in [2–4].

Let us consider the results of creating linac components as well resonator tuning and power load.

1. SUQF LINAC RESONATOR

In March 2015, the production division of the Zababakhin Institute of Technical Physics in Snezhinsk finished assembling the resonator of the SUQF linac, which consists of three sections. The resonator

was manufactured in two stages. First, the steel shells and electrodes of the resonator were made (see Fig. 1a). The electrodes were installed and aligned with a precision of $\pm 100 \mu\text{m}$. At the second stage, the inner surface and electrodes, except for their poles, of the resonator were coated with copper (see Fig. 1b). The thickness of the copper coating on the shells varied from 40 to 60 μm , and that on the electrodes was 37–40 μm . Copper coating was not applied to the poles of the electrodes because the modulation of the electrodes in the first section of the linac is $\sim 20 \mu\text{m}$.

Before the resonator was transported to the ITEP, where its testing and fine-tuning were scheduled, the main electrodynamic characteristics of the resonator were measured. The resonance frequency of the operating mode of the resonator without adjusting tools or power-input loop installed was $f_0 = 144.2 \text{ MHz}$ (the LU-20 operating frequency is 145.2 MHz), the unloaded quality factor was $Q_0 = 5300$, and the closest parasite (dipole) mode was $\Delta f \approx 10 \text{ MHz}$ from the operating mode frequency.

In order to prevent oxidation inside the resonator during its transportation to the ITEP, nitrogen was injected into the resonator to a pressure of 2 atm.

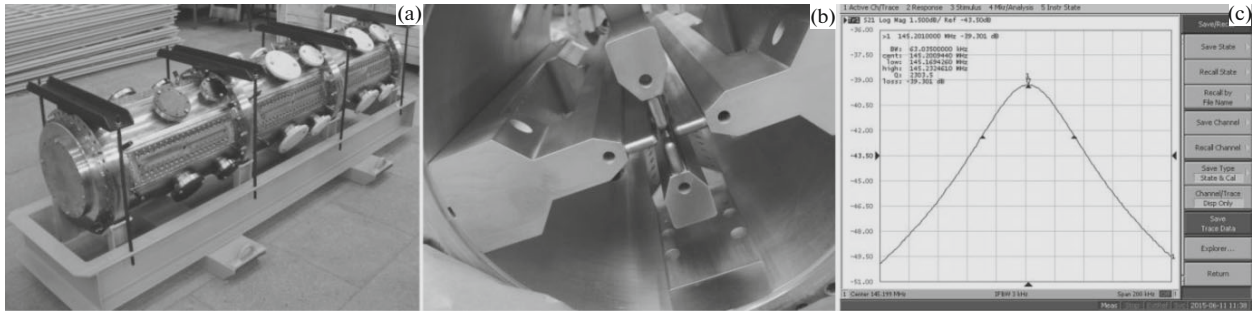


Fig. 1. Resonator before (a) and after (b) coppering; amplitude-frequency characteristic of the resonator after the electrodes have been polished (c).

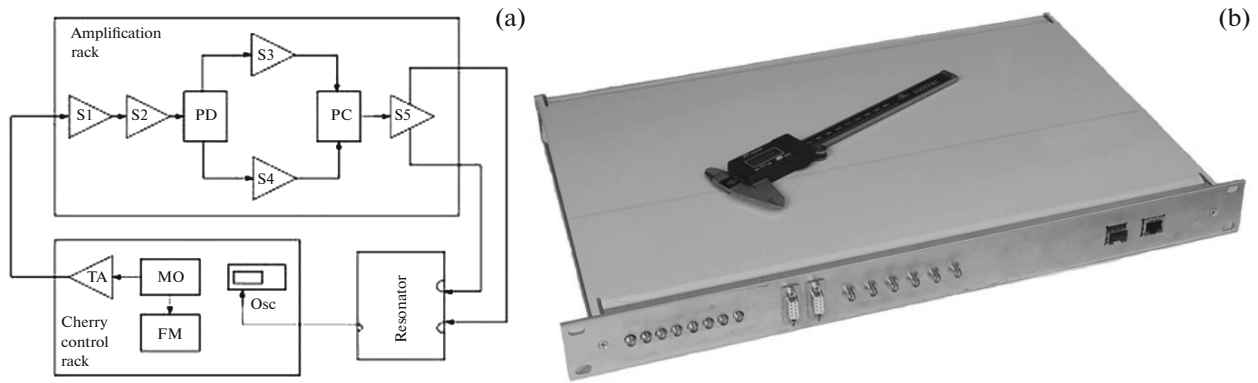


Fig. 2. Chart of the resonator excitation (a) and a photograph of the master generator (b): MG, master generator; TA, transistor amplifier; FM, frequency meter; Osc, oscilloscope; S1–S4, GI39B amplification stages; S5, GI17AM amplification stage.

2. RF SYSTEM

The RF power-supply system of the new RFQ section [3] is peculiar in the sense that it needs to be synchronized with the signal from the LU-20 accelerator, which operates in a self-excitation mode. The flow chart of the RFQ resonator excitation is presented in Fig. 2a. The reference RF signal from a master generator (MG) is fed to a solid-state amplifier and then to a preliminary amplification rack. The preliminary amplification rack consists of two series-connected amplification stages (S1 and S2), a power divider (PD), two in-parallel amplification stages (S3 and S4), and a power combiner (PC).

All the amplification stages in the rack are identical and built as grounded-grid circuits around GI39B oscillating tubes. The signal from the combiner is fed to the input of the final GI27AM-triode tube stage. The power from the final stage is finally supplied to the resonator itself via two RF feeders. In order to ensure synchronous operation of the RFQ section in a two-resonator setup, a master-oscillator module has been developed with functions of automatically adjusting the RFQ resonator's frequency and capturing the frequency and phase of the LU-20 resonator (Fig. 2b). Mechanical plungers allow one to synchronize the

RFQ and LU-20 frequencies within 10% of the RFQ resonator's frequency band, whereas the capture algorithm ensures synchronization of the frequencies and phases of two systems during the RF field rise period in LU-20. The operation of the RF generator is described in detail in [5].

3. FINE-TUNING THE RESONATOR AND RF POWER LOAD

Air-tightness tests were run on the resonator at the ITEP and revealed leaks at the junctions of resonator sections, as well as at the sites where butt flanges were installed. In order to ensure the working pressure ($<1 \times 10^{-6}$ mbar), vacuum sealing was enhanced by a gasket made of a vitone cord, 2 mm in diameter, that was installed above a contact copper-wire spacer. The RF power load was tried after a pressure of 8×10^{-7} mbar was achieved in the resonator. Two loops (see Fig. 3a) and two AFC plungers (Fig. 3b) were installed in the second section of the resonator for the RF power load. The AFC plungers were pulled out to half their excursion (the full excursion was 80 mm). The resonance frequency was $f_0 = 144.33$ MHz. When the RF power was loaded, it was discovered that RF breakdowns inside the structure render resonator

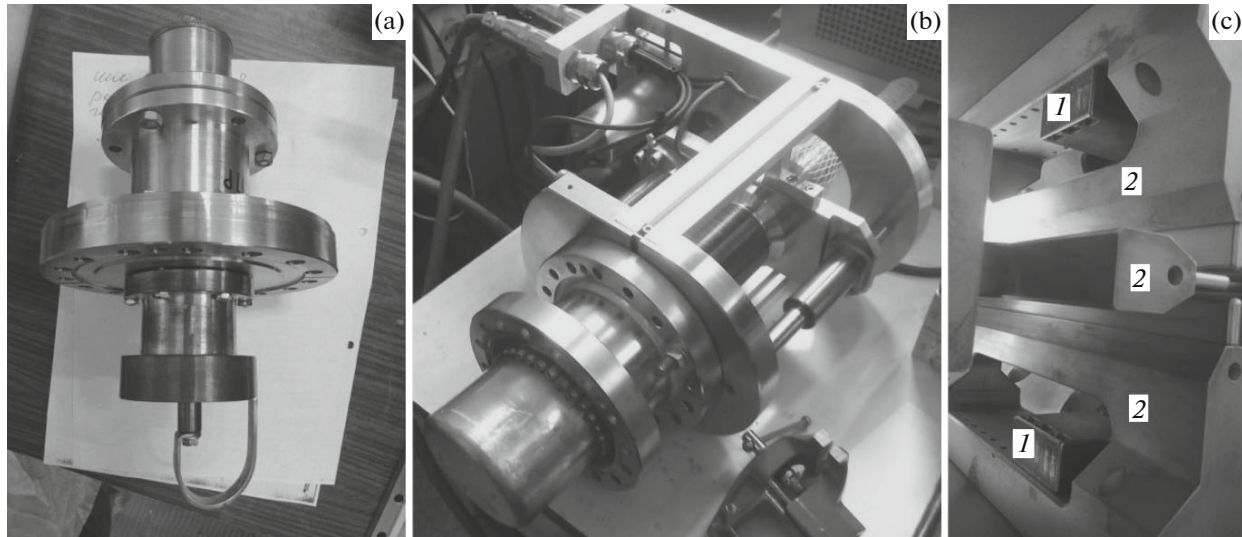


Fig. 3. Power load loop (a), AFC plunger (b), and electrode linings ((1) lining, (2) electrode) that are used to adjust the frequency (c).

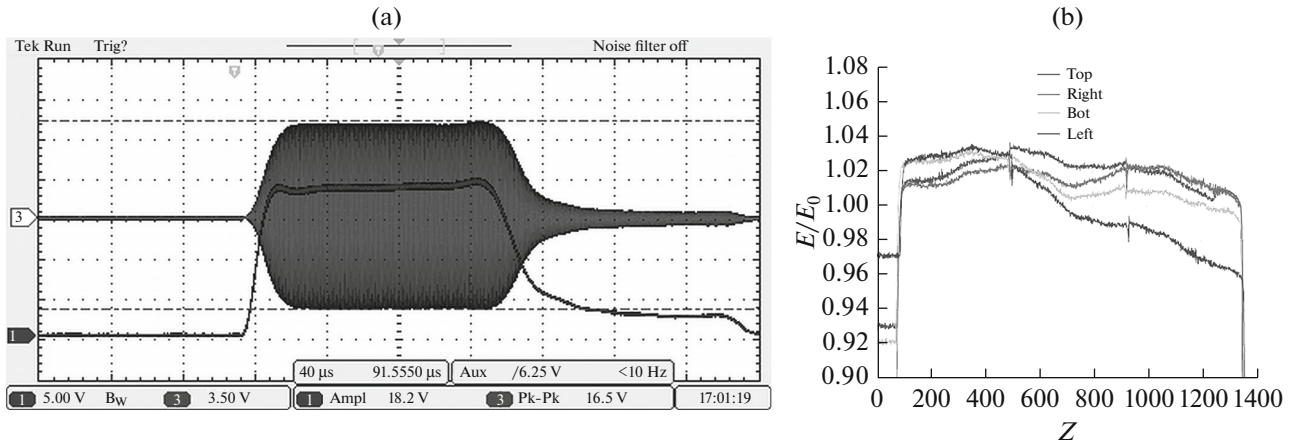


Fig. 4. Electric-field strength measured in the resonator quadrants (a) and oscillograms of the RF signal from the resonator and of the anode voltage pulse of high-frequency generator (b).

RF power loads of more than 200 kW impossible, and this value is only 60% of the value required for accelerating ions with $Z/A = 0.3$ level.

It has been found out that RF breakdowns occur between the electrodes, i.e., in maximum electric-field strength regions. On this basis, a conclusion has been drawn that the main reason is the roughness of the surface of electrode poles and its insufficient purity. The poles of the electrodes were then polished, and the RF power load resumed.

The measured tuning range in which the resonance frequency of the resonator was adjusted with the help of the AFC plungers (between two extreme positions of the plungers) was $\Delta f = 420$ kHz. Therefore, linings were installed into the coupling apertures of electrodes (see Fig. 3c) in order to tune the resonator to the required frequency 145.2 MHz (Fig. 1c) with the AFC plungers pulled half out of the excursion. Two linings on opposite electrodes were installed in each section.

A copper gasket 2 mm in diameter is installed along the perimeter of the lining's bottom surface to ensure reliable contact between the lining and an electrode leg. The linings are attached to electrodes with six bolts. Holes for the bolts are stretched-out, and this allows one to adjust the influence the linings have on the resonance frequency by moving the latter along the electrodes.

Measurements of the electric-field strength in the accelerator quadrants (Fig. 4a) have shown that the field inhomogeneity over the entire resonator length is no more than $\pm 2\%$.

The resonator was set for round-the-clock evacuation and, after a pressure of 8×10^{-7} mbar was achieved, the resonator's inner surface started to be aged, which continued for 2 weeks. By the end of the second week, a desired input-power level (Fig. 4b) of ≈ 340 kW was attained. This level corresponds to the electric field strength that is needed to accelerate ions

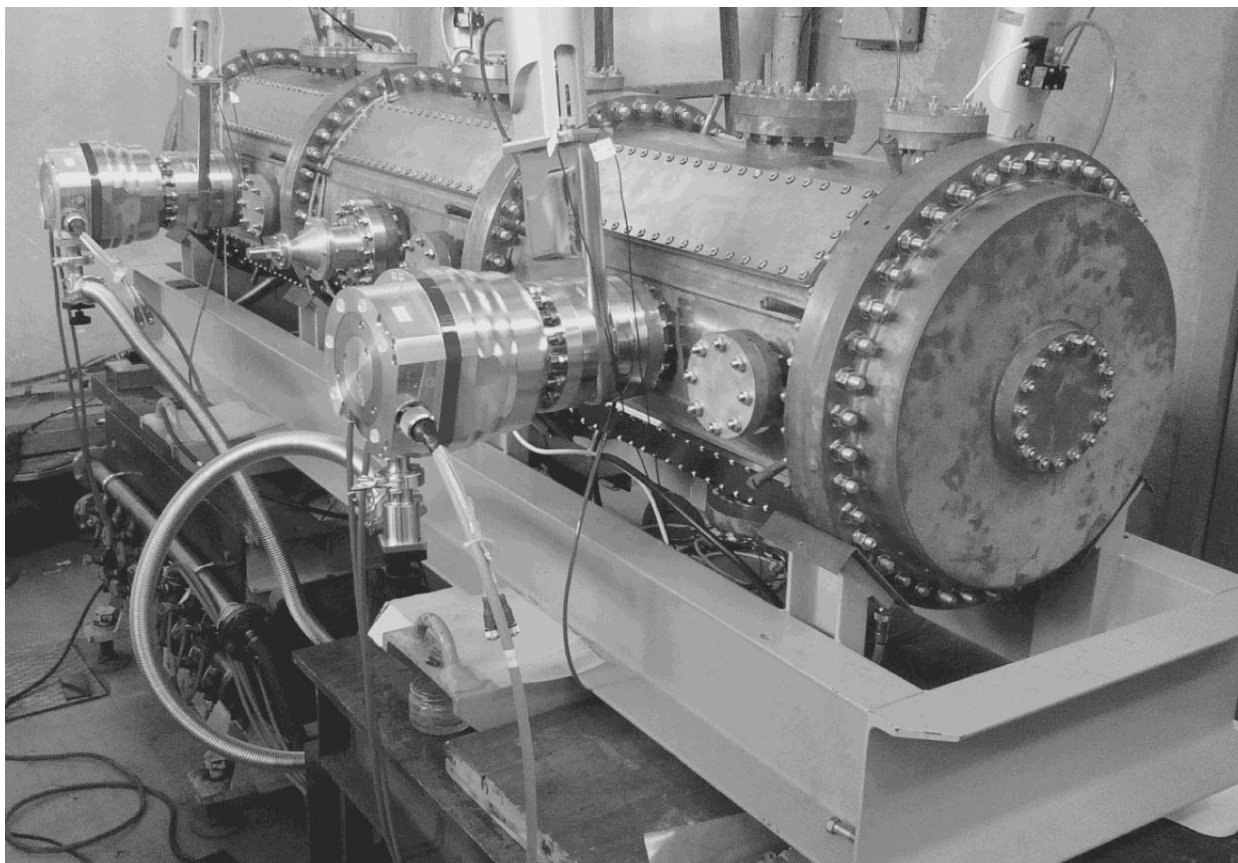


Fig. 5. Resonator of the RFQ accelerator with vacuum, RF, and measurement equipment mounted.

with $Z/A = 0.3$. By the time the aging finished, the residual pressure in the resonator was 3.8×10^{-7} mbar.

CONCLUSIONS

During the reconstruction of the system for proton and light-ion injection into the Nuclotron-NICA accelerator complex, the accelerating resonator of the RFQ section (Fig. 5) was mounted, tuned to the working frequency, and evacuated to the required vacuum. An RF power of about 340 kW, which is required for accelerating ions with $Z/A = 0.3$, was loaded into the resonator. The resonator and the RF power system are now being prepared for transportation to JINR.

REFERENCES

1. G. V. Trubnikov, N. N. Agapov, E. D. Donets, V. V. Fimushkin, E. V. Gorbachev, A. Govorov, E. V. Ivanov, V. Karpinsky, V. D. Kekelidze, H. G. Khodzhbagiyani, A. D. Kovalenko, K. A. Levterov, V. A. Matveev, I. N. Meshkov, V. A. Mikhailov, et al., "NICA project at JINR," in *Proceedings of the 4th International Particle Accelerator Conference IPAC'2013, Shanghai, China, May 12–17, 2013*, pp. 1343–1345.
2. A. V. Butenko, E. D. Donets, E. E. Donets, V. V. Fimushkin, A. I. Govorov, A. D. Kovalenko, K. A. Levterov, I. N. Meshkov, V. N. Monchinsky, A. Yu. Ramsdorf, A. O. Sidorin, G. V. Trubnikov, H. Hoeltermann, H. Podlech, U. Ratzinger, et al., "Development of the NICA injection facility," in *Proceedings of the 4th International Particle Accelerator Conference IPAC'2013, Shanghai, China, May 12–17, 2013*, pp. 3915–3917.
3. V. A. Andreev, A. I. Balabin, A. V. Butenko, V. S. Dyubkov, A. I. Govorov, B. V. Golovensky, V. V. Kobets, A. A. Kolomiets, V. A. Koshelev, A. D. Kovalenko, A. V. Kozlov, G. N. Kropachev, R. P. Kuibeda, T. V. Kulevoy, V. G. Kuzmichev, et al., "Reconstruction of light and polarized ion beam injection system of JINR Nuclotron-NICA accelerator complex," *Probl. At. Sci. Technol., Ser.: Nucl. Phys. Invest.*, No. 6 (88), 8–12 (2013).
4. A. V. Butenko, E. D. Donets, E. E. Donets, V. V. Fimushkin, A. I. Govorov, V. V. Kobets, A. D. Kovalenko, K. A. Levterov, I. N. Meshkov, V. N. Monchinsky, A. O. Sidorin, G. V. Trubnikov, A. S. Belov, T. V. Kulevoy, D. A. Lyakin, et al., "Development of NICA injection complex," in *Proceedings of the 5th International Particle Accelerator Conference IPAC'2014, Dresden, Germany, June 15–20, 2014*, pp. 2103–2105.
5. D. Liakin, S. Barabin, and A. Orlov, "Digital signal processing algorithms for LINAC low-level RF systems," in *Proceedings of the 24th Russian Particle Accelerator Conference RuPAC'2014, Obninsk, Russia, October 6–10, 2014* (JACoW, Geneva, 2014), pp. 392–394.

Translated by V. Potapchouck